[P5]

J. Villanen, J. Poutanen, C. Icheln, and P. Vainikainen, “A wideband study of the bandwidth, SAR and radiation efficiency of mobile terminal antenna structures,” *Proc. International Workshop on Antenna Technologies Conference (IWAT’07)*, Cambridge, UK, March 2007, pp. 49-52. 

# A Wideband Study of the Bandwidth, SAR and Radiation Efficiency of Mobile Terminal Antenna Structures

**J. Villanen, J. Poutanen, C. Icheln, and P. Vainikainen**

Helsinki University of Technology, IDC SMARAD/Radio Laboratory
P.O. Box 3000, FI-02015 TKK, Finland
Tel: +358 9 4512250, E-mail: juha.villanen@tkk.fi

**ABSTRACT:** In this paper, the frequency dependence of bandwidth, SAR and radiation efficiency of mobile terminal antennas are studied at wide frequency range, from 0.6 GHz to 6 GHz. Two antenna models are studied with simulations in free space and in talk-position beside a head model and two hand models. The results show a connection between chassis resonant frequencies, impedance bandwidth, SAR, and radiation efficiency. Increase in SAR and decrease in radiation efficiency occur when bandwidth reaches its maximum due to a chassis resonance. Above 3 GHz this trend is shown to be not valid anymore, as radiation of the antenna/coupling element become dominant. The results of the paper provide novel and useful information for the antenna designers of future mobile terminals.

## INTRODUCTION

Mobile terminals are required to operate in a growing number of communications systems. The most widely used cellular systems include GSM850/E-GSM900 (824 MHz – 960 MHz), GSM1800/PCS1900 (1710 MHz – 1990 MHz), and UTMS (1900 MHz – 2170 MHz). In the future, UMTS will be possibly extended to 2500 MHz – 2690 MHz. In addition, future mobile terminals need to be able to operate according to different WLAN standards. Currently WLAN works at the ISM band (2400 MHz – 2500 MHz) and also at the 5 GHz region (5150 MHz – 5825 MHz). As new system bands are taken into use, and the trend is towards thinner and more complex terminal devices, the role of antenna design is becoming more and more important. For an antenna designer, it would be especially useful to know and understand the general trends of impedance bandwidth, SAR and radiation efficiency of handset antenna structures at the wide frequency range of interest (0.8 GHz – 6 GHz). So far, only few studies have been published relating to this issue [1-3]. These studies present results on the bandwidth [1,2] and SAR [2,3] behavior of mobile terminal antennas at 900 MHz and 1800 MHz as a function of chassis length. According to [1,2], maximum impedance bandwidth is obtained when the electrical length of the chassis is close to half a wavelength. The results presented in [2] propose that SAR reaches its maximum at the chassis resonance. Opposite result was obtained in [3].

To the author's knowledge, there exist no wideband studies on the behavior of bandwidth and SAR of handset antennas as a function of frequency. Although the results presented in [1-3] are valuable and informative as such, they but cannot be directly used at other frequencies than 900 MHz and 1800 MHz. For example, material parameters of human tissue are frequency dependent, which should be taken into account if e.g. SAR is to be studied at wide frequency range. The purpose of this paper is to increase general understanding on the frequency behavior and trends of bandwidth, SAR and radiation efficiency of mobile terminal antennas. Two simple coupling element-based antenna structures [1,4] are studied by simulations from 0.6 GHz to 6 GHz. Bandwidth potentials of the antenna structures are first studied in free space. The results are then compared to surface integrals of chassis current distributions, which describe the amplitude of chassis characteristic wavemodes [5]. This is followed by a study in talk-position with a head model and two different hand models. Results are presented for bandwidth potential, chassis current integrals, SARs and radiation efficiencies. Finally, conclusions are given.

## SIMULATION METHODS AND MODELS

### General

An FDTD based commercial electromagnetic software SEMCAD X (version 10.0 EIGER) was used for the study. The input impedances of the coupling elements (described later), SARs, radiation efficiencies and chassis current distributions were simulated using a sinusoidal excitation and a frequency step of 100 MHz. The coupling elements were excited with a gap voltage source with a $50\,\Omega$ series source resistance. Medium-strength UPML boundaries were used to enclose the simulation space. The maximum cell size used inside antenna, head and hand models was $\Delta x = \Delta y = \Delta z = 2$ mm. The distance between the head model and the back-side surface of the chassis in the standard "cheek" position was 7 mm throughout the study. All presented SAR and radiation efficiency values are normalized to 1 W power accepted by the coupling elements. It should be noted that the specified mean antenna input powers for handsets in the GSM900, GSM1800 and UMTS systems are 250 mW, 125 mW and 250 mW, respectively.

1-4244-1088-6/07/$25.00 ©2007 IEEE.

**Head and Hand Models**

The head model used in the simulations was the SAM phantom model provided by SEMCAD. It consists of a thin shell and a homogenous brain-tissue-simulating liquid inside the shell. The dielectric parameters for the liquid were calculated as a function of frequency using parametric model by Gabriel et. al. [6]. The values of relative permittivity varied from 47.49 to 38.07 in the range of 0.6 GHz to 6 GHz. Correspondingly, effective conductivity varied from 0.66 S/m to 4.44 S/m. The density of the brain-tissue-simulating liquid in the simulations was 1040 kg/m$^3$.

Two different hand models were used in the work. Details of the hand models can be found from [2]. Hand model 1 models mainly the palm of a hand, while the fingers are very short. Distance between the palm and the chassis of a mobile terminal is only 2 mm, which makes the hand model a "worst case scenario". The palm of hand model 2 is identical to that of hand model 1 but the fingers are clearly longer. The thumb is holding one long side of the chassis and the rest fingers the other. In hand model 2, the distance from the chassis to the palm is 49.5 mm. Both hand models consists of two tissues, bone surrounded by muscle. The dielectric data across the frequency range for the hand models was calculated based on [6]. For bone, the relative permittivity varied from 17.18 to 12.41, while values for the effective conductivity were between 0.19 S/m and 1.72 S/m. For muscle, the corresponding values were 55.96 - 48.22 and 0.85 S/m - 5.20 S/m, respectively. Densities for bone and muscle were 1645 and 1050 kg/m$^3$, respectively.

**Antenna Models**

In this work, two coupling element based antenna structures were studied. The idea of coupling elements [1,4] suits well for purposes of the wideband study of this paper, as the fundamental idea is to use coupling elements that are not tuned to resonance at any specific frequency. Impedance matching at the desired frequency is done with a separate matching circuitry. For the purposes of this study, matching circuitries are not needed. Geometries of the studied antenna models are presented in Fig. 1. In antenna model 1, the coupling element is placed fully on top of the shorter end of the chassis. The coupling element of antenna model 2 is placed partly outside the perimeter of the chassis, and additionally bent over the end of the chassis to maximize coupling to the chassis wavemode, as described in [1,4]. The coupling elements of both antenna models occupy the same volumes (2.9 cm$^3$) and have same heights (6.6 mm). Voltage sources were placed on the 1 mm air gaps located between the feed pins and the upper surfaces of the ground planes. One should note that the general trends found in this paper should in principal also be valid with self-resonant antenna elements.

**FREE SPACE RESULTS**

**Bandwidth Potential and Chassis Current Distributions**

The first step was to study the effects of chassis resonances on the bandwidth potentials of the studied antenna structure. As post-processing, ideal lossless lumped elements were used to match the coupling elements at each simulated (SEMCAD) frequency point (see details from [4]). For each matching frequency, relative bandwidth ($|S_{11}| \leq$ -6 dB) was computed. Results for antenna model 1 and antenna model 2 in free space are presented in Fig. 2 (a). As can be seen from Fig. 2 (a), the relative bandwidth curves have local maxima located at chassis first, second, and third order resonant frequencies, as could be expected. From Fig. 2 (a) it can also be seen that the bandwidth potential of antenna model 2 is clearly larger than that of antenna model 1, as with antenna model 2 coupling to the chassis wavemodes is stronger. It was also considered interesting to study, how the amplitudes of chassis wavemodes behave as a function of frequency. This was done by computing surface integrals of simulated (SEMCAD) chassis currents over the lower half of chassis backside, as in [4]. The results were normalized to the surface integral calculated over the whole backside of the chassis. Normalized results are presented in Fig. 2 (b). According to Fig. 2 (b), the amplitudes of chassis wavemodes have local maxima at chassis resonant frequencies. As the frequency increases, chassis currents decrease

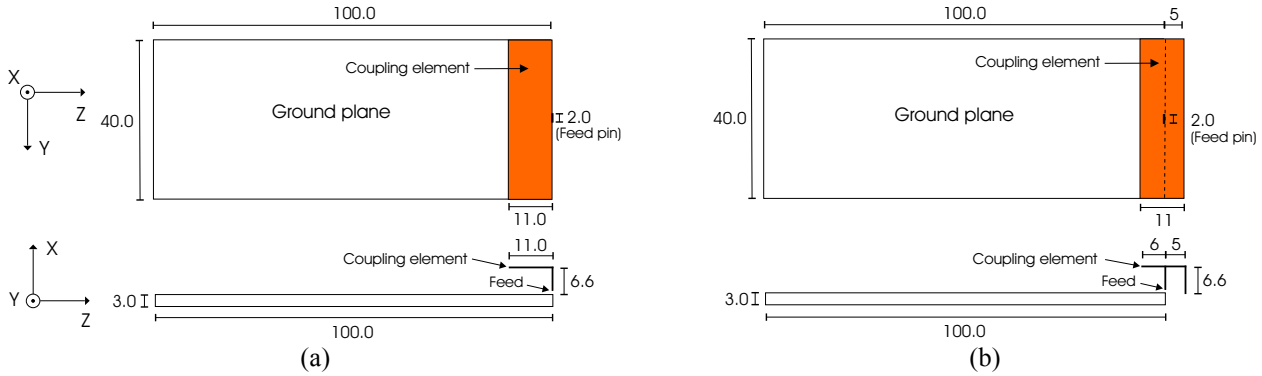


**Fig. 1. Geometries (in mm) of the studied antenna structures (a) antenna model 1 (b) antenna model 2.**

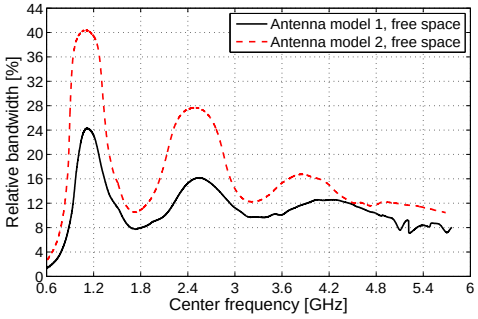


(a)

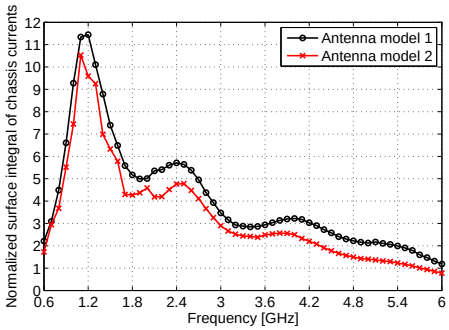


(b)

**Fig. 2. (a) Relative bandwidths ($|S_{11}| \leq$ -6 dB) and (b) normalized surface integrals of chassis current distributions as a function of frequency in free space.**

steadily. This is expected, as at higher frequencies the contribution of the wavemodes of the antenna/coupling element to the radiation increases [1]. The conclusion is also supported by Fig. 2 (a), in which the level of bandwidth peaks constantly decreases as frequency increases. One should note that the chassis currents of antenna model 2 are actually stronger than those of antenna model 1. This cannot be seen from Fig. 2 (b) due to the used normalization method.

## TALK-POSITION RESULTS

### Bandwidth Potential and Chassis Current Distributions

The bandwidth potentials obtained in talk-position with hand model 1 and hand model 2 are presented in Fig. 3 (a). As a general note, higher bandwidths are again obtained with antenna model 2. At higher frequencies the difference between antenna models becomes fairly small, as the chassis wavemodes do not contribute much anymore to radiation. With both antenna models, the first order resonant frequency of the chassis is clearly lower with hand model 1 (at around 0.9 GHz) than with hand model 2 (at around 1.2 GHz). This can be explained by the very short distance between the dielectric palm of hand model 1 and the chassis of the mobile terminal. The second order resonant frequency of the chassis, however, is not affected much by the type of the hand model. As an interesting observation, bandwidth potentials of both antenna models at the frequency range of about 1.4 GHz – 3.6 GHz are substantially higher in talk-position with the hand models than in free space. This can be seen by comparing the results in Fig. 2 (a) and Fig. 3 (a).

Normalized surface integrals of chassis current distribution in talk-position are presented in Fig. 3 (b). Again, it can be seen that the amplitudes of chassis wavemodes have maxima at chassis first order resonant frequencies, which depend on the type of the used hand model. At higher frequencies, the currents of the chassis wavemodes become very small.

### SAR and Radiation Efficiency

Fig. 4 shows the simulated radiation efficiencies and 10 g averaged SARs as a function of frequency. According to [2] the basic behaviour is that at chassis resonances, an increase in SAR and a decrease in radiation efficiency occur. The trend of SARs in the head model follows this rule up to about 3 GHz. At about 3 GHz, SARs in the head model start to increase. This can be expected to be caused by concentration of currents and electric near-fields to the region

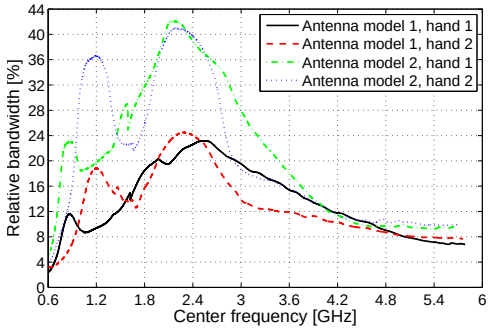


(a)

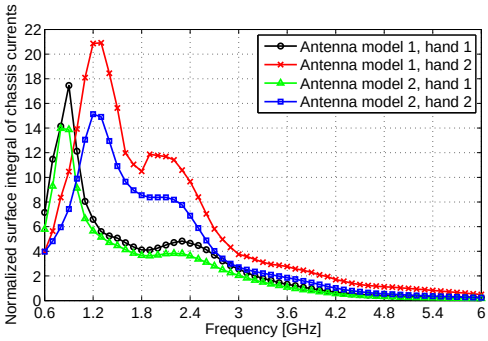


(b)

**Fig. 3. (a) Relative bandwidths ($|S_{11}| \leq$ -6 dB) and (b) normalized surface integrals of chassis current distributions as a function of frequency in talk-position with the hand models.**

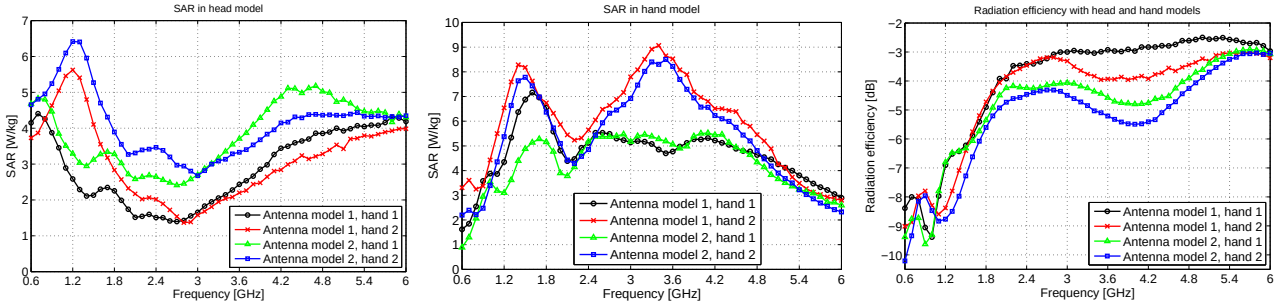


(a) (b) (c)

**Fig. 4. 10g averaged SARs and radiation efficiencies in talk-position as a function of frequency. (a) SAR in head (b) SAR in hand (c) radiation efficiency.**

of the coupling element as the characteristic wavemodes of the chassis become weaker. The conclusion is supported by the finding that above 3 GHz, SAR maximums in the head model were always located in the region under the coupling elements. At the chassis resonant frequencies below 3 GHz, SAR maximums in the head model were always located under the center part of the chassis. The SARs of antenna model 2 are clearly higher than those of antenna model 1 through the whole frequency range. Below 3 GHz this is expected, as coupling to the chassis wavemode is stronger with antenna model 2. Above 3 GHz, the higher SARs of antenna model 2 are most likely caused by the shaping of the coupling element. As the coupling element of antenna model 2 is bent towards the head of the user, the electric near-field components tangential to the surface of the head model are most likely higher than with antenna model 1.

From Figs. 3 (b) and 4 (b) no clear relation can be found between the amplitudes of chassis wavemodes and the SAR maxima in the hand models. At the first local SAR maxima around 1.4 - 1.5 GHz, SAR maxima in the hand models were located near the middle part of the chassis with both antenna models. At the second local SAR maxima around 3.4 GHz, SAR maxima were with both antenna models located at the thumb of hand model 2. One should note that similar second local SAR maxima are not present with hand model 1. Obviously, this issue requires further investigation. Above 3.5 GHz, the hand SARs decrease rapidly, as more and more power is lost to the head model due to increased radiation originated from the coupling elements.

The general trends in the radiation efficiencies presented in Fig. 4 (c) agree fairly well with the trends in head SARs in Fig. 4 (a). It can be seen that radiation efficiencies have their first minima at chassis first order resonant frequencies, around 1.2 GHz or 0.9 GHz depending on the hand model. After that, radiation efficiencies increase rapidly while head SARs decrease, as chassis wavemodes become weaker (see Fig. 3 (b)). Radiation efficiency maxima are obtained around 3 GHz, where head SARs reach their minimum. From 3 GHz to around 4.2 GHz, radiation efficiencies mostly decrease, while head SARs increase due to increased radiation from the coupling elements.

## CONCLUSIONS

This paper presents an extensive simulation study on the frequency dependence of bandwidth, SAR and radiation efficiency of mobile terminal antennas. Two coupling element based antenna structures are studied at the frequency range of 0.6 GHz – 6 GHz, both in free space and in talk-position with two different hand models. Clear connections between bandwidth, SAR and radiation efficiency are found. The results indicate that below 3 GHz, the main contributor on head SAR and radiation efficiency are chassis wavemodes. Above 3 GHz, the wavemodes of antenna/coupling element become dominant. The results of this paper provide useful information for antenna designers.

## REFERENCES


[1] P. Vainikainen, J. Ollikainen, O. Kivekäs and I. Kelander, ”Resonator-based analysis of the combination of mobile handset antenna and chassis”, *IEEE Transactions on Antennas and Propagation*, Vol. 50, No. 10, 2002, pp. 1433-1444.

[2] O. Kivekäs, J. Ollikainen, T. Lehtiniemi and P. Vainikainen, ”Bandwidth, *SAR*, and efficiency of internal mobile phone antennas”, *IEEE Transactions on Electromagnetic Compatibility*, Vol. 46, No. 1, 2004, pp. 71 - 86.

[3] D. Manteuffel, A. Bahr, D. Waldow, and I. Wolff, “Numerical analysis of absorption mechanisms for mobile phones with integrated multiband antennas”, *Proc. IEEE Antennas and Propagation Symp.,* 2001, pp. 82 - 85.

[4] J. Villanen, J. Ollikainen, O. Kivekäs and P. Vainikainen, ”Coupling element based mobile terminal antenna structures”, *IEEE Transactions on Antennas and Propagation*, Vol. 54, No. 7, July 2006, pp. 2142 - 2153.

[5] R. F. Harrington and J. R. Mautz, “Theory of characteristic modes for conducting bodies”, *IEEE Transactions on Antennas and Propagation*, Vol. 19, No. 5, September 1971, pp. 622-628.

[6] S. Gabriel, R.W. Lau and C. Gabriel, “The dielectric properties of human body tissues: III. Parametric models for the dielectric spectrum of tissues.” *Phys. Med. Biol.* 41 (1996), 2271-2293.